Engineering Targeted Near Infrared Emissive Polymersomes for Imaging Applications

by

Ruijuan Zhou

Department of Chemistry
Duke University

Date:_____
Approved:

_____
Michael J. Therien, Supervisor

_____
Stephen Craig

_____
Jiyong Hong

Thesis submitted in partial fulfillment of
the requirements for the degree of
Master of Science in the Department of
Chemistry in the Graduate School
of Duke University

2014

ABSTRACT

Engineering Targeted Near Infrared Emissive Polymersomes for Imaging Applications

by

Ruijuan Zhou

Department of Chemistry
Duke University

Date:_____
Approved:

_____
Michael J. Therien, Supervisor

_____
Stephen Craig

_____
Jiyong Hong

An abstract of a thesis submitted in partial
fulfillment of the requirements for the degree
of Master of Science in the Department of
Chemistry in the Graduate School of
Duke University

2014

Abstract

Interdisciplinary investigation at the interface of chemistry, engineering and medicine has triggered the development of self-assembled nanomaterials with novel biomaterial and optical properties. Targeted near infrared (NIR) emissive polymersomes can be used as agents of deep tissue fluorescent imaging and targeted drug delivery. For the development of these agents, my approaches were modification of polymersome surface with functional groups for protein conjugation, and optimization of NIR emissive fluorophores enhancing their organization homogeneity as well as increasing dispersion in polymersomes matrix. Results show successful protein conjugation to biodegradable polymersomes and thus a step forward to apply polymersomes for *in vivo* imaging and targeted drug delivery with low toxicity.

Contents

List of Tables

List of Figures

Acknowledgements

I would like to thank my advisor, Dr. Michael J. Therien, for the opportunity to work in his laboratory and the guidance he provided throughout this process.

I would also like to express my gratitude to the members of my thesis committee, Dr. Stephen Craig and Dr. Jiyong Hong for your time and commitment.

I would like to thank Dr. Wei Qi, for all her help, kindness and mentoring, leading me into the scientific research. Thanks also to all the members of the Therien Lab. I am grateful for your friendship, ideas and support.

I would also like to thank my collaborators for their ideas, work and support.

Finally, I would like to express my love to my family for all their support, encouragement and love during my four years of graduate study.

1. Introduction to near infrared emissive polymersomes in imaging applications and specific aims for the thesis

1.1 Introduction

Polymersomes (50 nm – 50 um diameter synthetic polymer vesicles) have attracted much attention in the studies of soft materials development because of their advantages in physical, optical and biomaterial properties[1] as well as promising clinical applications in deep tissue fluorescent imaging[2] and drug delivery[3]. Compared to liposomes, which have long been utilized to encapsulate aqueous soluble imaging and therapeutic agents, polymersomes exhibit their superior properties: 1) more chemically and mechanically stable by rational design of block copolymer compositions[4]; 2) further designed to degrade over longer timescales[2b]; 3) larger in size and hence having thicker[5] bilayer membranes which provides more probabilities of incorporating hydrophobic agents.

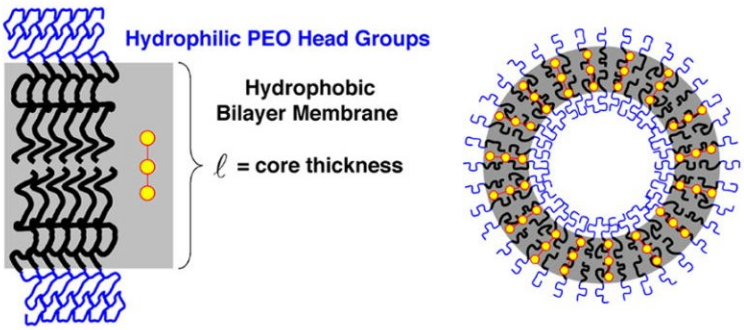

Figure 1: Polymersome structures. Illustration of PZn_3 dispersion within the vesicle's hydrophobic bilayer membrane.[6]

Amphiphilic block copolymers are obtained by the polymerization of more than one type of monomer, typically one hydrophobic and one hydrophilic, so that the resulting molecule is composed of regions that have opposite affinities for an aqueous solvent, which is a necessary property for their self-assembly into polymersomes[7].

Because of their unique amphiphilic structures, polymersomes can be modified in various ways such as designing of diblock copolymers, surface functionalization, incorporation of porphyrin - based near infrared (NIR) fluorophores (NIRFs)[8] into hydrophobic the bilayer membranes of these structure and encapsulation of hydrophilic chemicals into their inner aqueous core.

1.2 Specific Aims

My research on the targeted near infrared emissive polymersomes for imaging applications includes three specific aims.

1.2.1 Aim 1. Chapter 2. Optimization of near infrared emissive agents

Developing NIR emissive agents has become an interesting topic for their promising application for in vivo deep tissue imaging. Our group has developed polymer vesicles with porphyrin-based fluorophores incorporated as promising self-assembled nanomaterials[8-9]. Their impressive optical features are high emission oscillator strengths and high irradiance, and tunable physical and biomaterial characteristics relative to inorganic fluorescent nanoparticles[8]. However, NIR-emissive polymersomes can be further optimized to increase emissive intensity and

organizational homogeneity, therefore enhance signal to noise (SNR) for higher sensitivity of fluorescent imaging detection.

NIR-emissive polymersomes can be modulated in various ways. Previous studies have shown that membrane incorporation of multi-porphyrinic fluorophores through non-covalent interactions[10] has enabled precise emission energy modulation over a visible and near-infrared spectrum (600-900nm)[8]. Intramembranous polymer-fluorophore interactions can also be extensively modulated to influence the nature of fluorophore solvation, mean electronic environment and the porphyrin fluorophore (PZn) emission quantum yield, by the rational design of fluorophore ancilliary group substituents and the choice of polymer chain compositions[6].

The optimization of NIR-emissive polymersomes requires[6]:

1) elucidation of fluorophore photophysics in order to design emitters with appropriately large NIR extinction coefficients and fluorescence quantum yields;

2) regulation of the average fluorophore-fluorophore interspatial separations in order to facilitate fluorophore emission;

3) loading of appropriate numbers of fluorophores within a single vesicle composite in order to maximize signal sensitivity.

My research herein focused on the meso-to-meso ethynyl-bridged (porphyrinato)zinc(II)-based fluorophore and examine the effects of substituent-driven dispersion in PEO-PBD polymersomes, differing in membrane core thickness, via steady

state absorption and emission spectroscopies. By comparing each nanoscale compositions' integrated steady-state emission intensity as a function of membrane-loading concentration, I am intending to elucidate the role of polymer chain / fluorophore local solvation effects and non-covalent binding interactions in determining the optical properties of emissive polymersomes.

1.2.2 Aim 2. Chapter 3. Antibody conjugated polymersomes for active targeting applications in imaging and bio-assay

Based on functionalization techniques for direct conjugation of antibody to polymersomes surface, our group has created a universal method to make immunopolymersomes for tumor cell targeting and tracking. An approach to the applications of immunopolymersomes is to detect circulating tumor cells (CTCs) in metastatic prostate cancer. Detecting rare CTCs in complex blood samples is a major challenge[11], which requires an exceptionally specific and sensitive assay for discerning and capturing CTCs with high efficiency. The current method has its disadvantage of high false positive rate[12]. One key advantage of immunopolymersomes is to have a better sensitivity based on near infrared molecule imaging. And the distinctive immunopolymersomes eliminates the need for tedious separation procedures. A few different specific antibodies towards CTC cells such as EpCAM (epithelial cell adhesion molecule) antibody have been conjugated to the functionalized near infrared-emissive polymersomes (NIR-EPs) and used to detect prostate cancer tumor cells *in vitro*.

1.2.3 Aim 3. Chapter 4. Protein conjugation of functionalized biodegradable polymersomes

Focusing on the vesicle surface modifications, targeted multifunctional polymersomes define an important soft matter platform that could be utilized in targeted drug delivery and medical imaging. Strategies have been developed to functionalize the polymersomes surface for protein or peptide conjugation by non-covalent[13] and covalent binding methods[14]. These functionalized polymersomes[15] have the ability to bind specific peptides, proteins or antibodies, and thus can be targeted to specific cell surface receptors, which also provides a promising strategy to image cancer cells *in vivo* and ultimately provide targeted drug delivery. However, most of the studies focused on the non-biodegradable copolymers such as poly(ethylene oxide)-*b*-polybutadiene (PEO-*b*-PBD)[1c, 10a, 16], poly(ethylene oxide)-*b*-polyethylethylene (PEO-*b*-PEE)[16] and polystyrene-*b*-poly(ethylene oxide) (PS-*b*-PEO)[17]. Only a few biodegradable copolymers have been developed for in vivo medical application. Polymer structures are shown in Figure 2. Compared to biodegradable copolymers, poly(ethylene oxide)-*block*-polycaprolactone (PEO-*b*-PCL)[18] can form fully bioresorbable vesicles, leaving no potentially toxic byproducts upon their degradation. Both poly(ethylene oxide) (PEO) and polycaprolactone (PCL) homopolymers have previously been approved for human use by the United States Food and Drug Administration (FDA). Moreover, these bioresorbable vesicles, formed through spontaneous self-assembly of their pure

component amphiphile, have manufacturing advantages in terms of cost, tunability and safety[2b].

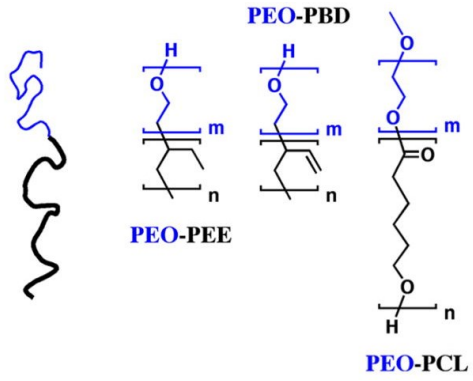

Figure 2: Chemical structures of biocompatible (PEO-b-PEE and PEO-b-PBD) and biodegradable (PEO-b-PCL) vesicle-generating diblock copolymers.[6]

My research on targeted polymersomes is focused on the vinyl sulfone functionalized poly(ethylene oxide)-*block*-poly (ε-caprolactone) (VS-OCL) polymersomes[19]. Like maleimide functional groups, vinyl sulfones can conjugate with thiol groups or cysteine-containing peptides. However, maleimide methods have some drawbacks: 1) maleimide is more reactive to thiols in aqueous solutions and thus provides an obstacle for *in vivo* applications[20]; 2) because of its reactivity, maleimide is typically purchased from commercial supplies and is accompanied by higher cost. Vinyl sulfone is therefore chosen as the functional group because of its advantages in low cost, stability in aqueous solutions and manageable reactions with biodegradable copolymers, which is necessary for successful development of a degradable, targeted drug delivery system.

2. Synthesis, characterization and properties of conjugated (porphinato)zinc(II) compounds featuring benzothiadiazole spacer units

2.1 Introduction

Imaging in the near infrared (NIR) region (700-110nm) has many advantages: lowest absorption of the major absorbers in tissues such as oxyhemoglobin and deoxyhemoglobin; decreased light scattering compared to visible region; outstanding signal-to-background ratio of fluorescence and the availability of low-cost source of irradiation.[2c]

A series of conjugated (porphinato)zinc(II) complexes with a spacer group Benzothiadiazole (BTD) were synthesized and characterized in the group[10b]. Generally, these BTD conjugated porphyrin compounds emit in the NIR region, possess high oscillator strength and large NIR fluorescence quantum yields of 17%-38% in THF. [21]

However, these chromophores are not ideal for use in polymersomes because of their 2′,6′-substituted aryl groups.

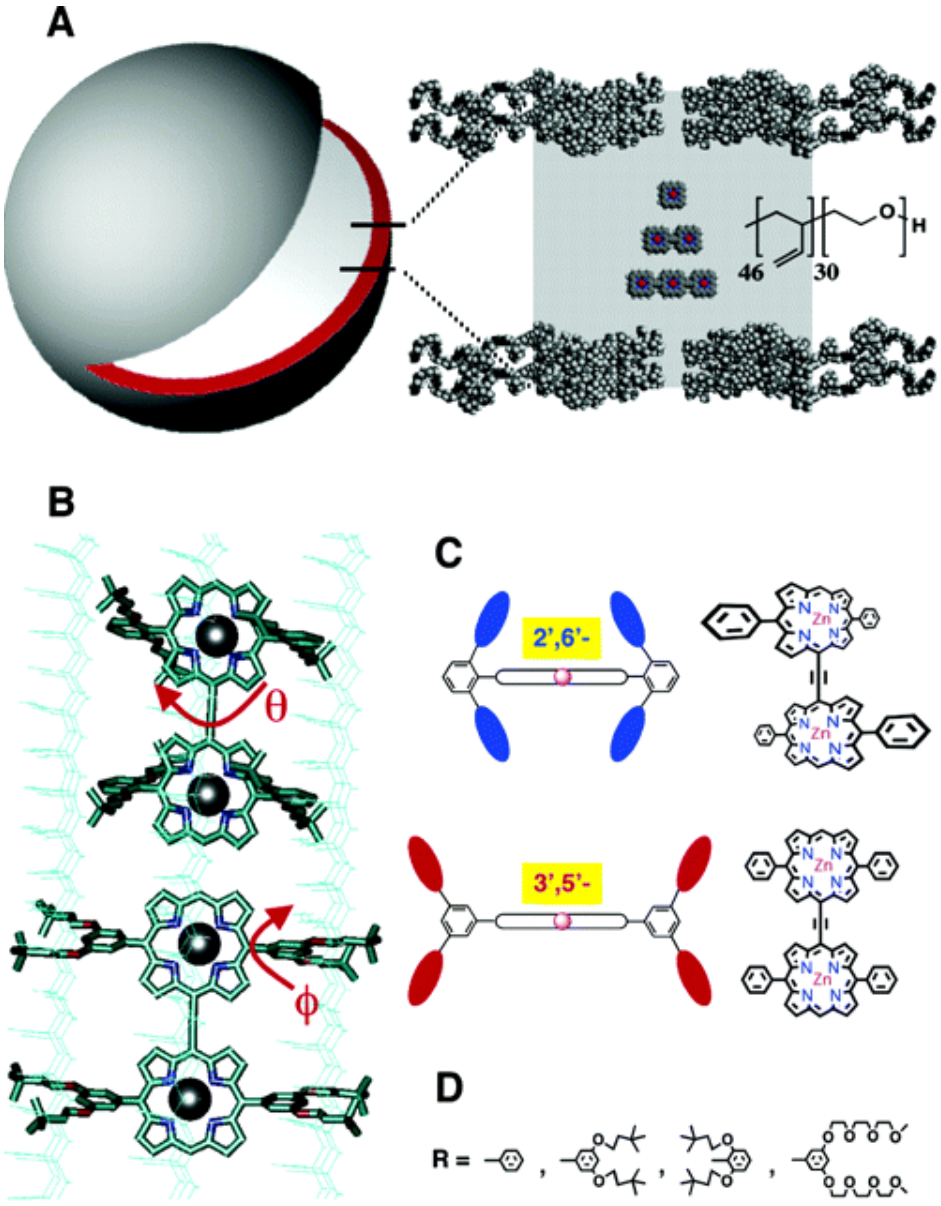

Figure 3: (A) Schematic of polymersomes incorporating mono-, bis-, and tris(PZn)-based chromophores. (B) Schematic representation of the interactions that modulate the degree of supermolecular conjugation, and the distribution and relative population of specific torsional angles for a given aryl-substituted multi(PZn)-based fluorophore; (θ) porphyrin-to-porphyrin interplanar torsional angle; (φ) torsional angle between the macrocycle core and the 10- and 20-pendant aryl groups. (C) Topological properties of 3',5'- versus 2',6'-substituted ethynyl-bridged bis(PZn) arrays. (D) Meso-phenyl ancillary substituents.[10b]

As described by Ghoroghchian, *et al.*(2005), in dilute THF solution, the position of the ancillary aryl 3,3-dimethyl-1-butyloxy substituent does not impact fluorophore optical properties; chromophores based on 10,20-diarylporphyrins having 2′,6′-disubstituted aryl rings exhibit the same absorptive and emissive signatures as those that feature 3′,5′-disubstituted meso-aryl groups. However, in polymersome environments, chromophores bearing 2′,6′-di(3,3-dimethyl-1-butyloxy)phenyl rings display fluorescence band blue shifts, while the same chromophores possessing a 3′,5′-aryl substitution pattern exhibit red shifted emission bands relative to that observed in THF solvent.[10b]

The nature of intermembranous polymer to fluorophore interactions depends on the position and identity of the porphyrins' phenyl ring substituents. The diminished freedom of polymer chains within the bilayer controls packing and characteristic chromophore solvation. The polymersome membrane not only defines a dielectric environment for these fluorophores that differs from bulk organic solvent but also impacts the magnitude of the porphyrin to porphyrin interplanar torsional angle as well as the extent of conjugation between the macrocycle core and the 10- and 20- pendant aryl groups. As shown in Figure 3, varying aryl group substitution from a 3′,5′- to a 2′,6′- pattern converts overall chromophore geometry from a biconcave wedge to a cylinder; these substantive gross structural modifications, coupled with the selection of

specific meso-phenyl ancillary substituents, influence the local arrangement of polymer chains.[10b]

The interactions of the chromophores' meso-aryl ring solubilizing substituents with polymer chains in the vesicles' bilayer membranes afford further modulation of their optical properties. Thus instead of the previous 2',6'-aryl substituents, here the research is focusing on synthesis the BTD spaced porphyrins bearing 3',5'- aryl substituents, to further optimize NIR emissive polymersomes with increased emissive intensity and organizational homogeneity for higher sensitivity of fluorescence imaging detection.

2.2 Conjugated (porphinato)zinc(II) compounds featuring benzothiadiazole spacer units

2.2.1 Synthesis of zinc porphyrin monomer

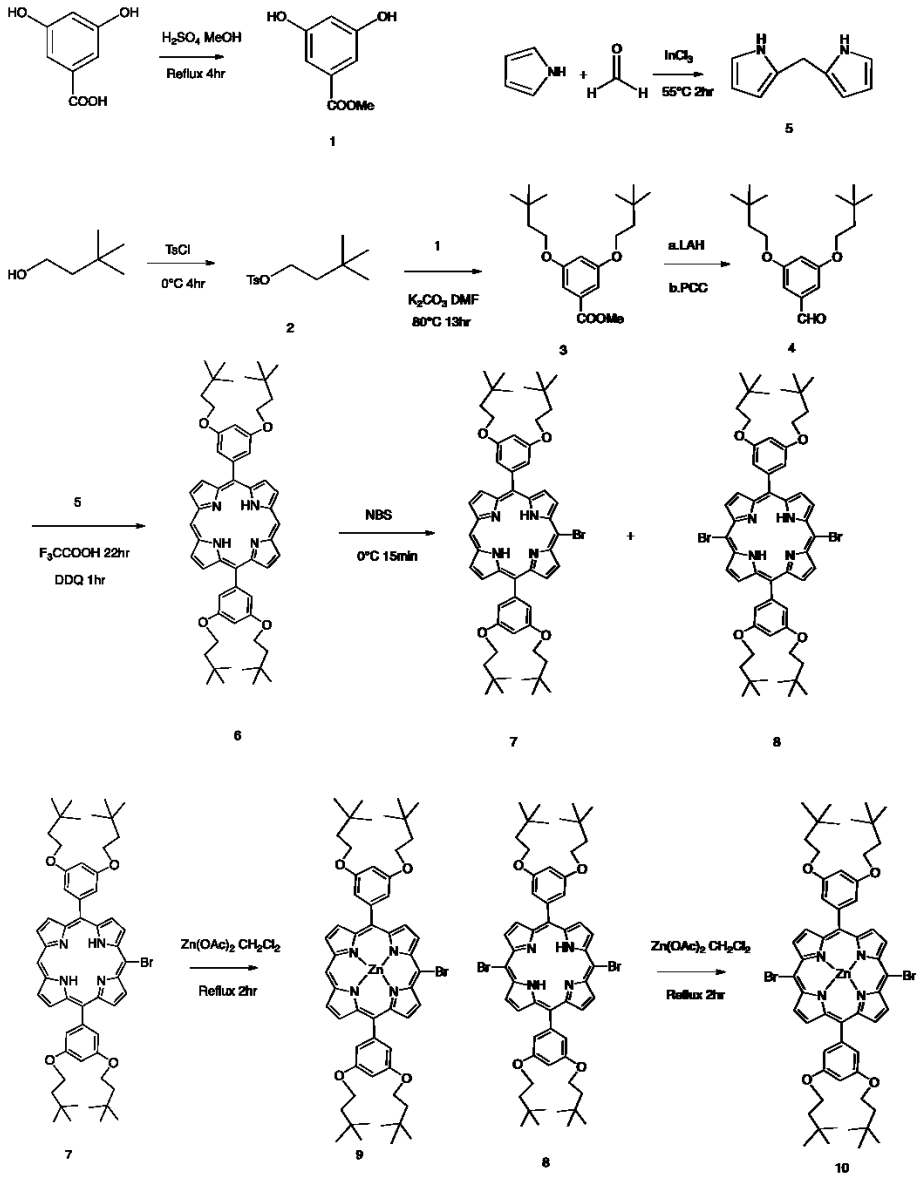

Figure 4: Scheme of zinc porphyrin monomer synthesis[8d]

2.2.2 Synthesis of PZn-BTD-PZn (DA) and PZn-BTD-PZn-BTD-PZn (TA)

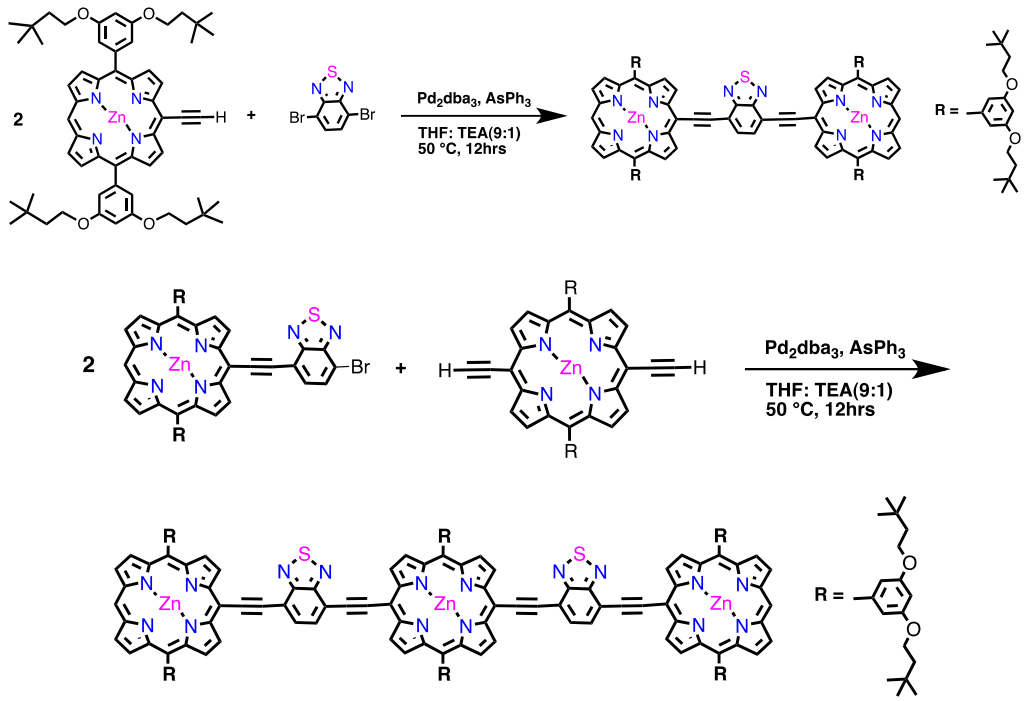

Figure 5: Scheme of BTD compound synthesis, DA and TA [21]

Synthesis of zinc porphyrin monomer from starting materials were carried out by previously reported procedures[8d] (Figure 4). Synthesis of BTD spacer compounds with 3′5′- aryl substituents were performed following the scheme in Figure 5, similarly to the procedures used to make BTD spacer compounds with 2′,6′- aryl substituents[21].

2.2.3 Spectroscopic properties of DA and TA

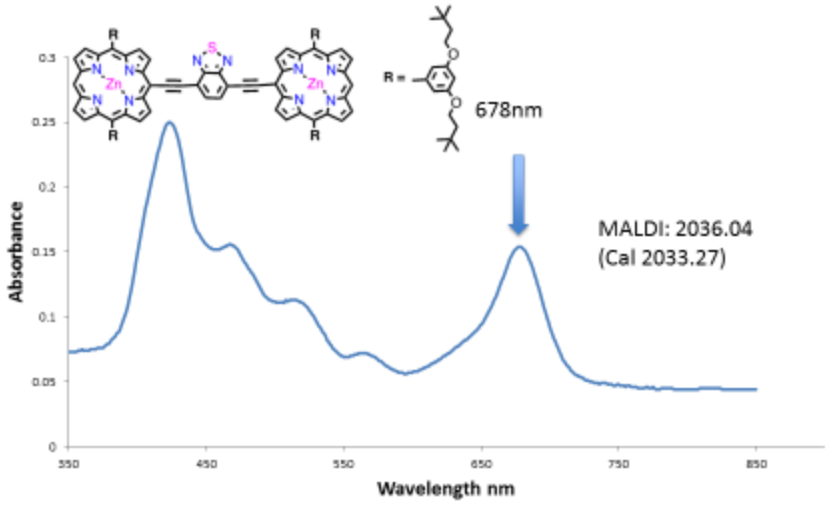

Figure 6: Absorption Spectra of DA in THF

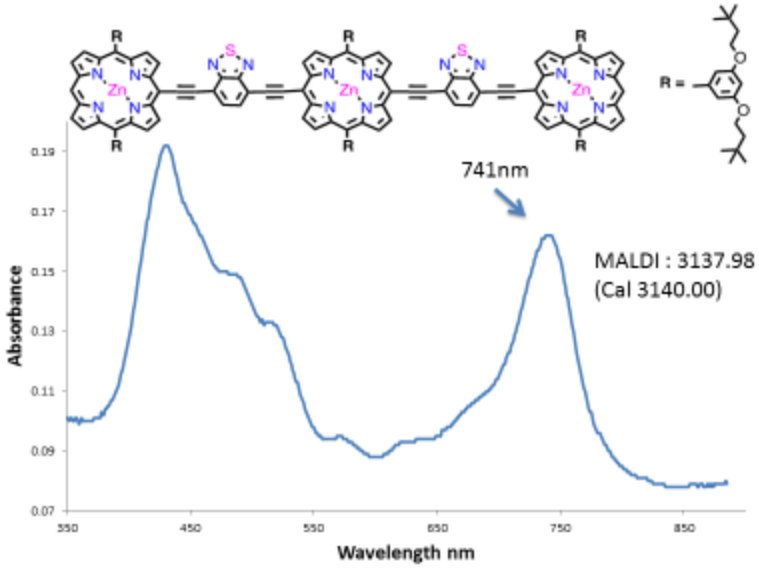

Figure 7: Absorption Spectra of TA in THF

Previous work has been done in the group on synthesis and characterization of conjugated (porphinato)zinc(II) complexes with an induced spacer group

benzothiadiazole (BTD) that regulate frontier orbital energy levels and progressively increase the extent of the quinoidal resonance contribution to the ground and electronically excited states, augmenting the magnitude of electronic communication and optimizing their optical properties in the near infrared region. [21] However, they (BTD spaced Tet zinc porphyrins) are not proper for polymersome incorporation because of aggregation and the steric effect of the 2,6 –bis(3,3-dimethyl-1-butyloxy)phenyl side chain.

Studies on porphyrin side chain effects on polymersome incorporation have indicated that 3,5-bis(3,3-dimethyl-1-butyloxy) phenyl side chains give better emission properties in polymersomes. Thus my work focuses on the synthesis of a series of BTD spaced conjugated (porphinato)zinc(II) complexes with 3,5-bis(3,3-dimethyl-1-butyloxy)phenyl side chains (BTD spaced Su zinc phorphyins). Molecules made are shown in Figure 6 (DA) and Figure 7 (TA). Each molecule was characterized by ^{1}H-NMR, MS, and absorption spectroscopy. The quantum yield of DA was tested by relative method[22]. DA quantum yield is 0.25, referenced by DD (ethynyl bridged porphyrin dimer without BTD spacer) quantum yield (0.16). Emission spectra shows about 27 nm red shift of Su version DA molecule (734 nm) relative to DD emission (707 nm), which indicates the probability of good incorporation properties of Su version BTD spaced porphyrins.

2.2.4 Selected NMR characterization of (porphinato)zinc(II) compounds

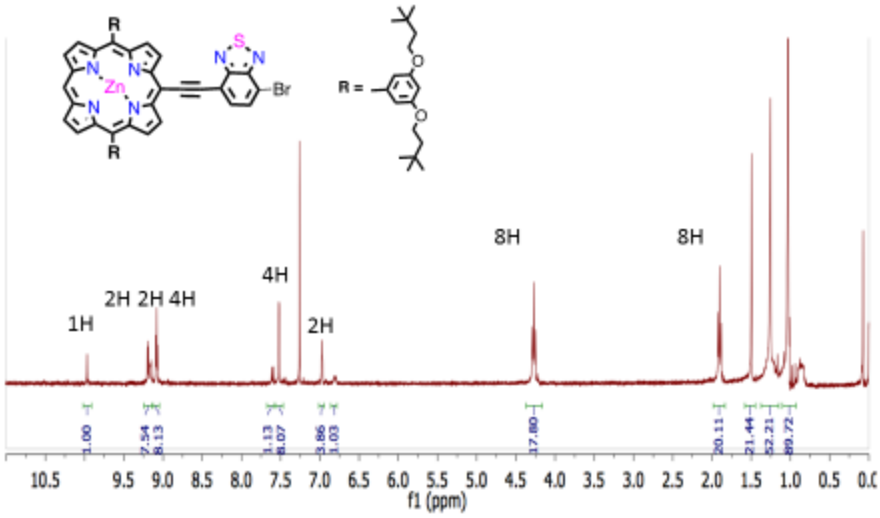

Figure 8: ^{1}H-NMR of Br-BTD-PZn

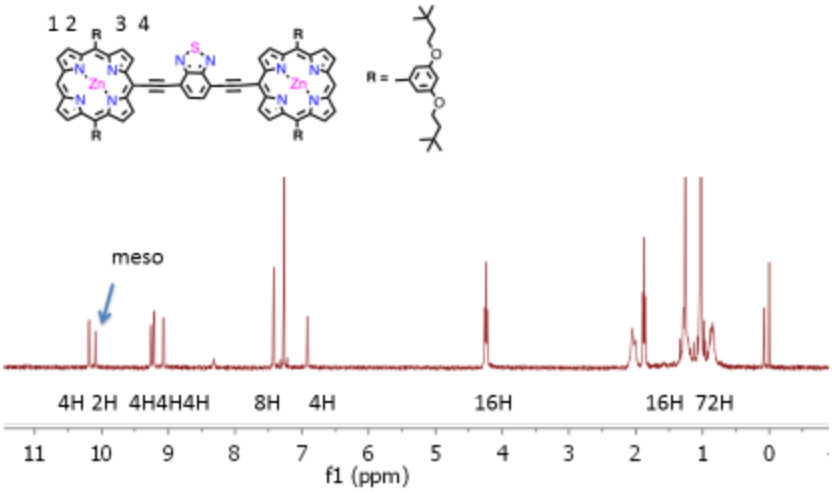

Figure 9: ^{1}H-NMR of DA compound

More selected ^{1}H-NMR of zinc porphyrin compounds were shown in the Appendix A.

3. Targeted near infrared emissive polymersomes

3.1 Introduction

Based on functionalization techniques for direct conjugation of antibody to polymersomes surface, our group has created a universal method to make immunopolymersomes for tumor cell targeting and tracking. An approach to the applications of immunopolymersomes is to detect circulating tumor cells (CTCs) in metastatic prostate cancer. Detecting rare CTCs in complex blood samples is a major challenge[11], which requires an exceptionally specific and sensitive assay for discerning and capturing CTCs with high efficiency. The current method has its disadvantage of high false positive rate[12]. One key advantage of immunopolymersomes is to have a better sensitivity based on near infrared molecule imaging. And the distinctive immunopolymersomes eliminates the need for tedious separation procedures. A few different specific antibodies towards CTC cells such as EpCAM have been conjugated to the functionalized NIR-emissive polymersomes and used to detect prostate cancer tumor cells *in vitro*.

3.2 Methods and materials

3.2.1 Polymersome preparation protocol

Maleimide functionalized PEO(3600)-*b*-PBD(6800) diblock copolymer is mixed with PEO(1300)-*b*-PBD(2500) diblock copolymer at a mole ratio of 5:95. The mixed diblock copolymer and porphyrin fluorophore dimer (PZn_3) were dissolved in

methylene chloride at a 40:1 molar ratio of polymer to NIRF. The solution was then plated onto a roughened Teflon film and dried under vacuum overnight. Polymersomes were formed upon the addition of 290 mOsm pH 4 MES buffer solution sonicated (1 h) in a bath sonicator. A narrow size distribution of nano-sized polymersomes was achieved with serial extrusion using a Liposofast Basic hand-held extruder equipped with 400-, 200- and 100-nm polycarbonate membranes (Avestin Inc., Ottawa, Ontario).

EpCAM antibody (Abcam, USA) was thiolated with 2-iminothiolane. 2-iminothiolane was dissolved at 2mg/ml in PH 8 sodium borate buffer containing 3mM EDTA. The molar ratio of 2-iminothiolane added to antibody was 20:1. The reaction was performed at RT for 1 hour under Ar. Proceed to desalt the SH-modified antibody into conjugation buffer (pH 7.4, PBS buffer). The pH of the preformed maleimide functionalized polymersomes was adjusted to pH 7.0 by adding NaOH (1M). The thiolated antibody was incubated with the maleimide functionalized polymersomes overnight with stirring under Ar flow at room temperature. The reaction mixture was then applied to a sephacryl S-500 HPLC column and eluted with 0.01 M PBS buffer (pH 7.4). The EpCAM antibody to polymersome coupling efficiency was quantified by BCA protein assay.

3.2.2 Flow cytometry

BD FACS CANTO II flow cytometer (BD biosciences) was employed to determine the fluorescence intensity achieved by near infrared emissive polymersome

uptake by corresponding cell lines. Cells were gated by the forward versus side scattering parameters and all experiments analyzed a minimum of 10 000 cell events. The near infrared fluorophores (PZn_3, maximum emission 810nm) were excited using an argon ion laser (488nm) and probed with fluorescence detection of Cy7 channel (>790nm). Polymersomes concentration was 2nM unless further specified. Raw data were analyzed based on the mean fluorescence intensity of gated cells using flowjo software.

Experimental diagram is shown in Figure 10.

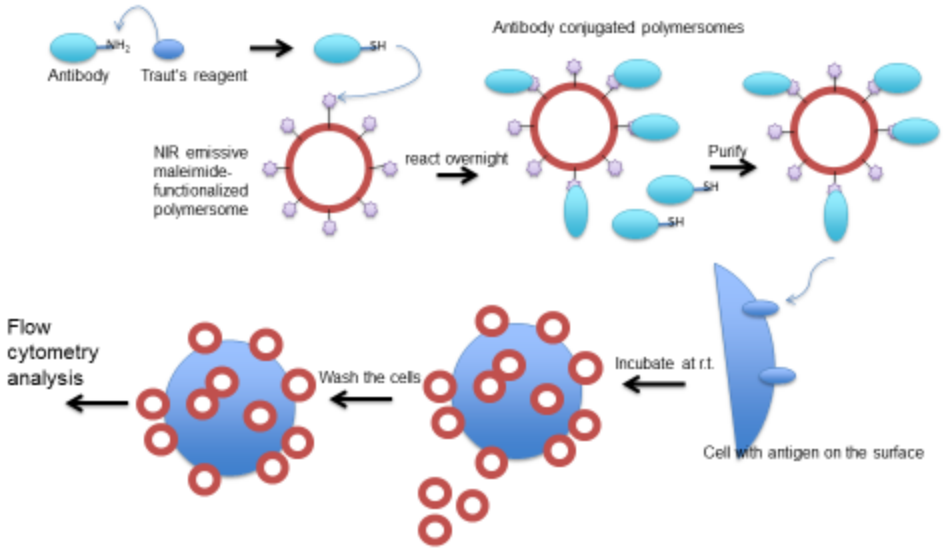

Figure 10: Diagram for antibody conjugation to polymersomes and cell incubation with antibody conjugated NIR emissive polymersomes.

3.3 Results and discussion

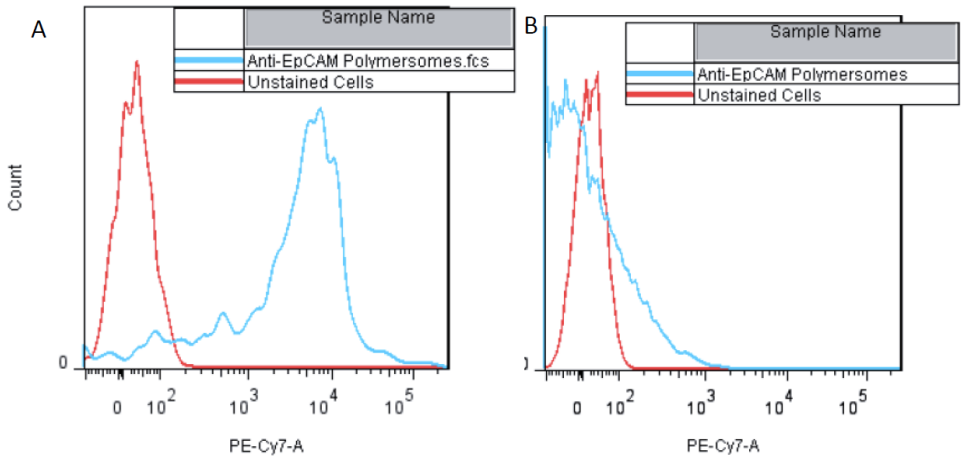

Figure 11: Flow analysis of anti-EpCAM polymersome staining with T47D cells (left) and PBMC cells (right)

Flow sorting shown in Figure 11, using the EpCAM conjugated near infrared emissive polymersomes (NIR-EPs), demonstrates clear signal separation of T47D cells (left) versus unstained cells using the Cy7 (>790nm) channel. Peripheral blood mononuclear cells (PBMCs) that lack EpCAM demonstrate very little nonspecific binding (right).

Results show the flow cytometry analysis of anti-EpCAM polymersomes incubated with T47D (human ductal breast epithelial tumor cell line) cells, which highly express EpCAM (Epithelial cell adhesion molecule), and PBMC cells, which do not express EpCAM as negative control. With 2nM immunopolymersome concentration, the flow data indicate that EpCAM positive cells (T47D) can be 100% stained with anti-EpCAM polymersomes.

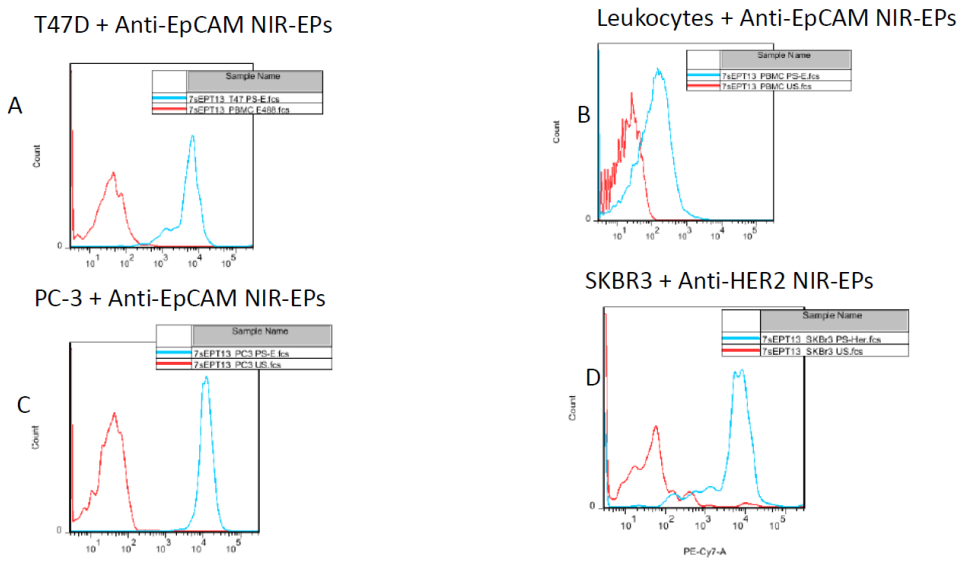

Figure 12: Evaluation of two antibody conjugated NIR-EPs: anti-EpCAM polymersomes and anti-Her2 polymersomes

Based on previous results. More cell lines and antibody were utilized for the validation of conjugation efficiency and the potential for bioassay applications. Figure 12 A), B) indicates the consistent results with Figure 11, anti-EpCAM polymersomes stained specifically to T47D cells, while they demonstrate little nonspecific binding to PBMC cells. In C), PC-3 cells also stained positively with anti-EpCAM polymersomes. And Figure 12 D) shows specific binding of anti-HER2 polyersomes to the HER2 positive SKBR3 cells. Flow cytometry analysis were taken using the Cy7 (>790nm near infrared wavelength) channel. Further optimization of antibody conjugated polymersomes protocol and flow cytometry instrumental settings are necessary for reproducibility before the technique to be applied into cell detection.

4. Biodegradable PEO-PCL Polymersomes

4.1 Introduction

Poly(ethylene oxide)-*block*-polycaprolactone (PEO-*b*-PCL)[18] can promise to form fully bioresorbable vesicles, leaving no potentially toxic byproducts upon their degradation. Both poly(ethylene oxide) (PEO) and polycaprolactone (PCL) homopolymers have previously been approved for human use by the United States Food and Drug Administration (FDA). Moreover, these bioresorbable vesicles, formed through spontaneous self-assembly of their pure component amphiphile, have manufacturing advantages in terms of cost, tune and safety.

Vinyl sulfone is chosen as the functional group because of its advantages for low cost, stability in aqueous solutions and manageable reactions with biodegradable copolymers, which is necessary for successful development of a degradable, targeted drug delivery system.

4.2 Methods and materials

4.2.1 Polymersome preparation

Thin film hydration method was employed to assemble functionalized VS-PEO-*b*-PCL copolymers into vesicles as described[16]. In brief, 1mM VS-PEO-*b*-PCL polymer with 2.5 mol% porphyrin was uniformly coated on the surface of Teflon plate, following which the solvent was evaporated under vacuum for >12h. Addition of PBS and heating at 60 °C for 48 h led to giant (5-20 μm) polymersomes in solution.

Small (<300 nm diameter) unilamellar polymersomes that process narrow size distributions were prepared via procedures analogous to those used to formulate small lipid vesicles (sonication, freeze-thaw extraction, and extrusion). The size distributions of PEO-*b*-PCL suspensions were determined in each case by dynamic light scattering (DLS).

4.2.2 Protein modification

BSA was dissolved into aqueous phosphate buffered saline (PBS) buffer (5 mM EDTA, pH 8.0). Traut's reagent was then added into the solution by 40:1 ratio to BSA protein. The solution was incubated at room temperature for an hour, following which separating thiolated protein form excess Traut's Reagent using 40k desalting column (ThermoScientific) that has been equilibrated with buffer containing 5mM EDTA.

4.2.3 Protein conjugation to VS-OCL polymersomes

VS-functionalized polymersomes were reacted with thiolated BSA (1:1 mole ratio) overnight and then separated by HPLC to eliminate the excess unbound BSA. The fraction of BSA-modified polymersomes was then concentrated to 1.5 ml, followed by measurement of concentration. The concentration of the conjugated BSA was determined by BCA assay, while the polymersome concentration was measured by NIRF absorptions.

4.2.4 Cryo-TEM characterization

Samples were prepared within a controlled environment vitrification system (Vitrobot FEI Mark III, Hillsboro, OR). A droplet of solution (5 μl) was deposited on a copper TEM grid coated with a polymer film. A thin film (<300 nm) was obtained by blotting with filter paper. After allowing the sample sufficient time to relax from any residual stresses imparted during blotting, the grid was cooled in liquid ethane at its freezing point, resulting in vitrification of the aqueous film. Sample grids were examined in a transmission electron microscope (FEI Tecnai G2 Twin, Hillsboro, OR) operating at 200 kV, and images were recorded with a multiscan digital camera (Gatan 724).

4.2.5 Dynamic light scattering (DLS)

Light scattering instrument (DynaPro, Wyatt Technology, Santa Barbara, CA) was used to measure the hydrodynamic radius of prepared vesicles. Cuvette were filled with 10 μl of polymersomes suspensions diluted with 300 μl DI water and were thermostatically controlled at 25 °C throughout the experiment. Data analysis was performed using DYNAMICS software (Wyatt Techonology).

4.2.6 Quantification of protein—BCA assay

Bicinchoninic acid (BCA) protein assay (ThermoScientific) is used to quantify the extent of protein coupling to the polymersomes. First, we constructed a protein calibration curve by preparing a serial dilution of BSA in PBS and analyzing each

solution for protein content, with the BCA protein assay kit. Next, the protein concentration of BSA-conjugated polymersomes sample is measured by using BCA assay.

4.3 Results

Table 1: VS-functionalized polymer composition

Polymer	PEO (NMR) Weight fraction %	Vinyl Sulfone mole ratio %
VS-PEO(2K)-PCL(7.8K)	20.4	63.4
VS-PEO(2K)-PCL(8.5K)	19.0	70.2
VS-PEO(2K)-PCL(9.4K)	17.5	62.0
VS-PEO(2K)-PCL(10.0K)	16.7	67.7
VS-PEO(2K)-PCL(11.7K)	14.6	61.5
VS-PEO(2K)-PCL(14.1K)	12.4	62.9

After making assemblies of above VS-OCL polymer series using thin film hydration method, we check the morphology by Cryo-TEM. VS-PEO (2K)-b-PCL (10K) can form over 90% polymersomes.

To study protein conjugation to VS-OCL polymersomes, a blend of VS-PEO (2K)-*b*-PCL (10K) with PEO (2K)-*b*-PCL (12K) was used to prepare 100 nm-sized functionalized polymersomes at different functionalization degree (1 %-5 %). Next, thiolated BSA was added at 1: 1 molar ratio. Results are shown in Figure 13.

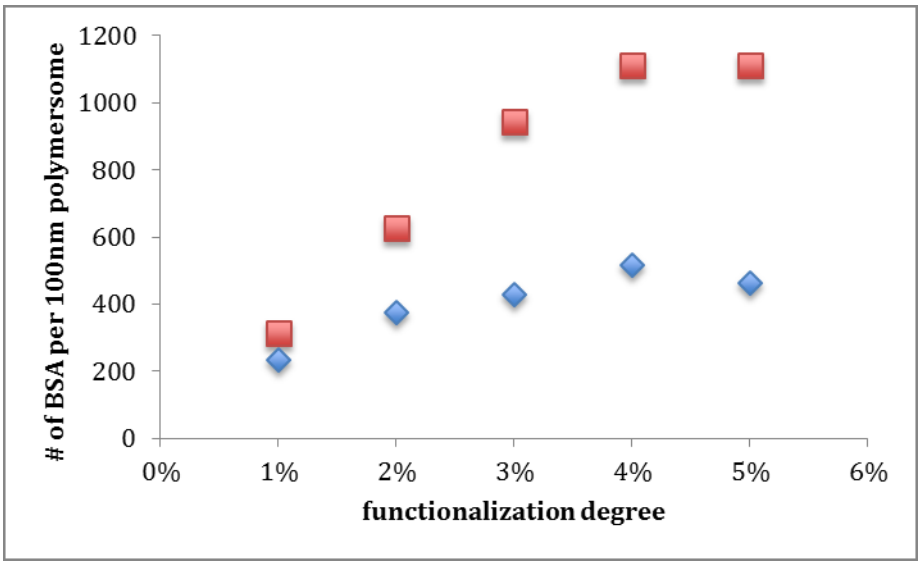

Figure 13: BSA conjugation with VS functionalized polymersomes compared with theoretical calculations. Polymersomes containing 1 to 5 mole% VS-functionalized polymer were incubated with BSA protein at a protein to functionalized polymer ratio of 1:1. Blue dots stand for experiment data of BSA conjugation; red dots stand for theoretical calculation.

We could calculate the maximum functionalization degree and number of protein per 100 nm polymersomes assuming BSA protein are spherical particles on polymersomes surface. Considering the diameter of BSA protein is about 6 nm, the projected area of BSA on polymersomes surface is 28.3 nm^2. The surface area of 100 nm polymersomes is 31400 nm^2, therefore the maximum number of BSA per 100 nm polymersomes is 1111 and the corresponding maximum functionalization degree is 3.5 %. Considering the steric hindrance effect on the polymersomes surface, the experimental numbers will be much smaller than these theoretical calculated numbers. Our measured values of conjugated BSA numbers were also with the same trend with theoretical calculated numbers.

4.4 Discussions

Previous research has shown that PEO (2K)-*b*-PCL (12K) diblock copolymers can self-assembly into polymersomes. Therefore we predict among those VS-functionalized polymers, VS-PEO (2K)-*b*-PCL (11.7K) is more likely to form polymersomes due to its similar weight fractions with PEO (2K)-*b*-PCL (12K). However, as it turned out, VS-PEO (2K)-*b*-PCL (10K) was our best candidate. From this phenomenon, we can confirm that vinyl sulfone functional group does influence the properties for polymer assembly.

In the protein conjugation test, BSA amounts were determined by comparison to absorption of calibration curves containing known amounts of protein. As it showed in results section, containing a thiol-bearing cysteine residue, low concentrations of protein were highly reactive, and nearly all of the protein coupled to vinyl sulfone groups on the surface of polymersomes. As the amount of protein was increased, the amount of coupled protein gradually plateaued at slightly over 40% of all vinyl sulfone groups. This is consistent with the fact that only outwardly oriented vinyl sulfone groups are available for reaction with thiols, as about half of the polymer chains of the polymersome matrix are situated on the inner surface of the polymersomes and thus inaccessible to proteins. Some amount of vinyl sulfone groups were not reactive probably because they were hydrolyzed or deep buried in the polymer chains, and the measured level of protein attachment is consistent with saturation or near-saturation of remaining reactive sites. In high protein concentration samples, unreacted vinyl sulfone

on the vesicle surface is likely because of increasing density following protein attachment and the steric restraints hindered the addition of proteins[14b].

Moreover, the experiment of BSA conjugation with VS-functionalized polymersomes shows the same trend with theoretical calculation, which is consistent with our expectation and also shows that the functionalization of biodegradable polymer is effective.

Appendix A

Selected ^{1}H-NMR for PZn_3 compound synthesis

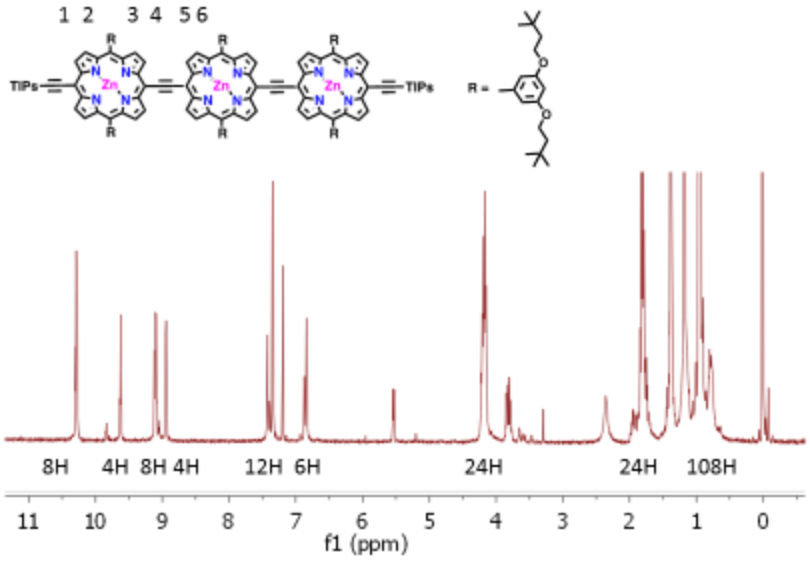

Figure 14: ^{1}H-NMR for PZn_3 compound with ethynyl end groups

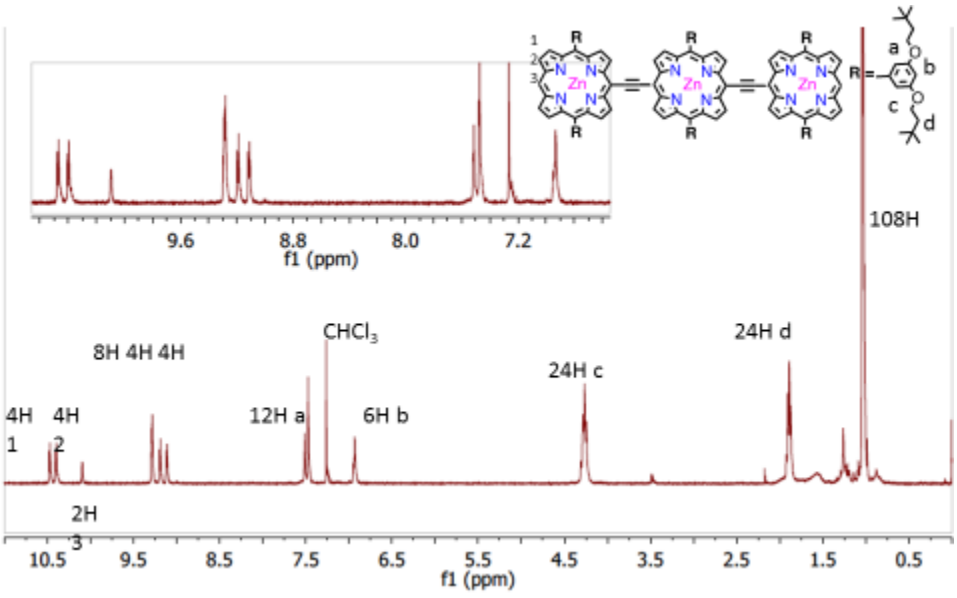

Figure 15: ^{1}H-NMR for PZn_3 compound

References

1. (a) Cornelissen, J.; Fischer, M.; Sommerdijk, N.; Nolte, R. J. M., Helical superstructures from charged Poly(styrene)-Poly(isocyanodipeptide) block copolymers. *Science* **1998,** *280* (5368), 1427-30; (b) Discher, B. M.; Won, Y. Y.; Ege, D. S.; Lee, J. C. M.; Bates, F. S.; Discher, D. E.; Hammer, D. A., Polymersomes: Tough vesicles made from diblock copolymers. *Science* **1999,** *284* (5417), 1143-1146; (c) Discher, D. E.; Eisenberg, A., Polymer vesicles. *Science* **2002,** *297* (5583), 967-73; (d) Antonietti, M.; Forster, S., Vesicles and liposomes: A self-assembly principle beyond lipids. *Adv Mater* **2003,** *15* (16), 1323-1333; (e) Opsteen, J. A.; Cornelissen, J. J. L. M.; van Hest, J. C. M., Block copolymer vesicles. *Pure Appl Chem* **2004,** *76* (7-8), 1309-1319.

2. (a) Sevick-Muraca, E. M.; Houston, J. P.; Gurfinkel, M., Fluorescence-enhanced, near infrared diagnostic imaging with contrast agents. *Curr Opin Chem Biol* **2002,** *6* (5), 642-50; (b) Ghoroghchian, P. P.; Li, G. Z.; Levine, D. H.; Davis, K. P.; Bates, F. S.; Hammer, D. A.; Therien, M. J., Bioresorbable vesicles formed through spontaneous self-assembly of amphiphilic poly(ethylene oxide)-block-polycaprolactone. *Macromolecules* **2006,** *39* (5), 1673-1675; (c) Ghoroghchian, P. P.; Therien, M. J.; Hammer, D. A., In vivo fluorescence imaging: a personal perspective. *Wires Nanomed Nanobi* **2009,** *1* (2), 156-167.

3. (a) Duncan, R., The dawning era of polymer therapeutics. *Nat Rev Drug Discov* **2003,** *2* (5), 347-60; (b) Uchegbu, I. F., Pharmaceutical nanotechnology: polymeric vesicles for drug and gene delivery. *Expert Opin Drug Deliv* **2006,** *3* (5), 629-40; (c) Upadhyay, K. K.; Bhatt, A. N.; Mishra, A. K.; Dwarakanath, B. S.; Jain, S.; Schatz, C.; Le Meins, J. F.; Farooque, A.; Chandraiah, G.; Jain, A. K.; Misra, A.; Lecommandoux, S., The intracellular drug delivery and anti tumor activity of doxorubicin loaded poly(gamma-benzyl L-glutamate)-b-hyaluronan polymersomes. *Biomaterials* **2010,** *31* (10), 2882-92; (d) Broz, P.; Benito, S. M.; Saw, C.; Burger, P.; Heider, H.; Pfisterer, M.; Marsch, S.; Meier, W.; Hunziker, P., Cell targeting by a generic receptor-targeted polymer nanocontainer platform. *J Control Release* **2005,** *102* (2), 475-488.

4. Bermudez, H.; Brannan, A. K.; Hammer, D. A.; Bates, F. S.; Discher, D. E., Molecular weight dependence of polymersome membrane structure, elasticity, and stability. *Macromolecules* **2002,** *35* (21), 8203-8208.

5. Photos, P. J.; Bacakova, L.; Discher, B.; Bates, F. S.; Discher, D. E., Polymer vesicles in vivo: correlations with PEG molecular weight. *J Control Release* **2003,** *90* (3), 323-334.

6. Ghoroghchian, P. P.; Frail, P. R.; Li, G. Z.; Zupancich, J. A.; Bates, F. S.; Hammer, D. A.; Therien, M. J., Controlling bulk optical properties of emissive polymersomes through intramembranous polymer-fluorophore interactions. *Chem Mater* **2007,** *19* (6), 1309-1318.

7. Kita-Tokarczyk, K.; Grumelard, J.; Haefele, T.; Meier, W., Block copolymer vesicles - using concepts from polymer chemistry to mimic biomembranes. *Polymer* **2005,** *46* (11), 3540-3563.

8. (a) Lin, V. S. Y.; Dimagno, S. G.; Therien, M. J., Highly Conjugated, Acetylenyl Bridged Porphyrins - New Models for Light-Harvesting Antenna Systems. *Science* **1994,** *264* (5162), 1105-1111; (b) Lin, V. S. Y.; Therien, M. J., The role of porphyrin-to-porphyrin linkage topology in the extensive modulation of the absorptive and emissive properties of a series of ethynyl- and butadiynyl-bridged bis- and tris(porphinato)zinc chromophores. *Chem-Eur J* **1995,** *1* (9), 645-651; (c) Rubtsov, I. V.; Susumu, K.; Rubtsov, G. I.; Therien, M. J., Ultrafast singlet excited-state polarization in electronically asymmetric ethyne-bridged bis[(porphinato)zinc(II)] complexes. *J Am Chem Soc* **2003,** *125* (9), 2687-96; (d) Susumu, K.; Therien, M. J., Decoupling optical and potentiometric band gaps in pi-conjugated materials. *J Am Chem Soc* **2002,** *124* (29), 8550-2.

9. Christian, N. A.; Milone, M. C.; Ranka, S. S.; Li, G.; Frail, P. R.; Davis, K. P.; Bates, F. S.; Therien, M. J.; Ghoroghchian, P. P.; June, C. H.; Hammer, D. A., Tat-functionalized near-infrared emissive polymersomes for dendritic cell labeling. *Bioconjug Chem* **2007,** *18* (1), 31-40.

10. (a) Ghoroghchian, P. P.; Frail, P. R.; Susumu, K.; Blessington, D.; Brannan, A. K.; Bates, F. S.; Chance, B.; Hammer, D. A.; Therien, M. J., Near-infrared-emissive polymersomes: self-assembled soft matter for in vivo optical imaging. *Proc Natl Acad Sci U S A* **2005,** *102* (8), 2922-7; (b) Ghoroghchian, P. P.; Frail, P. R.; Susumu, K.; Park, T. H.; Wu, S. P.; Uyeda, H. T.; Hammer, D. A.; Therien, M. J., Broad spectral domain fluorescence wavelength modulation of visible and near-infrared emissive polymersomes. *J Am Chem Soc* **2005,** *127* (44), 15388-90.

11. Kaiser, J., Medicine. Cancer's circulation problem. *Science* **2010,** *327* (5969), 1072-4.

12. (a) Panteleakou, Z.; Lembessis, P.; Sourla, A.; Pissimissis, N.; Polyzos, A.; Deliveliotis, C.; Koutsilieris, M., Detection of circulating tumor cells in prostate cancer patients: methodological pitfalls and clinical relevance. *Molecular medicine* **2009,** *15* (3-4), 101-14; (b) Maheswaran, S.; Haber, D. A., Circulating tumor cells: a window into cancer biology and metastasis. *Current opinion in genetics & development* **2010,** *20* (1), 96-9; (c) Pantel, K.; Brakenhoff, R. H.; Brandt, B., Detection, clinical relevance and specific

biological properties of disseminating tumour cells. *Nature reviews. Cancer* **2008,** *8* (5), 329-40.

13. Weber, P. C.; Ohlendorf, D. H.; Wendoloski, J. J.; Salemme, F. R., Structural origins of high-affinity biotin binding to streptavidin. *Science* **1989,** *243* (4887), 85-8.

14. (a) Pang, Z. Q.; Lu, W.; Gao, H. L.; Hu, K. L.; Chen, J.; Zhang, C. L.; Gao, X. L.; Jiang, X. G.; Zhu, C. Q., Preparation and brain delivery property of biodegradable polymersomes conjugated with OX26. *Journal of Controlled Release* **2008,** *128* (2), 120-127; (b) Petersen, M. A.; Yin, L. G.; Kokkoli, E.; Hillmyer, M. A., Synthesis and characterization of reactive PEO-PMCL polymersomes. *Polym Chem-Uk* **2010,** *1* (8), 1281-1290.

15. Egli, S.; Schlaad, H.; Bruns, N.; Meier, W., Functionalization of Block Copolymer Vesicle Surfaces. *Polymers* **2011,** *3* (1), 252-280.

16. Lee, J. C. M.; Bermudez, H.; Discher, B. M.; Sheehan, M. A.; Won, Y. Y.; Bates, F. S.; Discher, D. E., Preparation, stability, and in vitro performance of vesicles made with diblock copolymers. *Biotechnol Bioeng* **2001,** *73* (2), 135-145.

17. (a) Yu, K.; Eisenberg, A., Bilayer morphologies of self-assembled crew-cut aggregates of amphiphilic PS-b-PEO diblock copolymers in solution. *Macromolecules* **1998,** *31* (11), 3509-3518; (b) Yu, K.; Zhang, L. F.; Eisenberg, A., Novel morphologies of "crew-cut" aggregates of amphiphilic diblock copolymers in dilute solution. *Langmuir* **1996,** *12* (25), 5980-5984; (c) Yu, K.; Eisenberg, A., Multiple morphologies in aqueous solutions of aggregates of polystyrene-block-poly(ethylene oxide) diblock copolymers. *Macromolecules* **1996,** *29* (19), 6359-6361.

18. (a) Allen, C.; Han, J. N.; Yu, Y. S.; Maysinger, D.; Eisenberg, A., Polycaprolactone-b-poly(ethylene oxide) copolymer micelles as a delivery vehicle for dihydrotestosterone. *Journal of Controlled Release* **2000,** *63* (3), 275-286; (b) Sinha, V. R.; Bansal, K.; Kaushik, R.; Kumria, R.; Trehan, A., Poly-epsilon-caprolactone microspheres and nanospheres: an overview. *Int J Pharm* **2004,** *278* (1), 1-23; (c) Coombes, A. G. A.; Rizzi, S. C.; Williamson, M.; Barralet, J. E.; Downes, S.; Wallace, W. A., Precipitation casting of polycaprolactone for applications in tissue engineering and drug delivery. *Biomaterials* **2004,** *25* (2), 315-325; (d) Shenoy, D. B.; Amiji, M. A., Poly(ethylene oxide)-modified poly(epsilon-caprolactone) nanoparticles for targeted delivery of tamoxifen in breast cancer. *Int J Pharm* **2005,** *293* (1-2), 261-270.

19. Zupancich, J. A.; Bates, F. S.; Hillmyer, M. A., Synthesis and Self-Assembly of RGD-Functionalized PEO-PB Amphiphiles. *Biomacromolecules* **2009,** *10* (6), 1554-1563.

20. Roberts, M. J.; Bentley, M. D.; Harris, J. M., Chemistry for peptide and protein PEGylation. *Adv Drug Deliver Rev* **2002,** *54* (4), 459-476.

21. Therien, M. J.; Susumu, K., Novel conjugated materials featuring proquinoidal units. Google Patents: 2007.

22. Fery-Forgues, S.; Lavabre, D., Are Fluorescence Quantum Yields So Tricky to Measure? A Demonstration Using Familiar Stationery Products. *Journal of Chemical Education* **1999,** *76* (9), 1260.

23. Dr. Wei Qi, Dissertation Thesis, 2011